

Apparent horizontal displacements in time-lapse seismic images

Dave Hale^{*1}, Barbara Cox² and Paul Hatchell²

¹Center for Wave Phenomena, Colorado School of Mines

²Shell International E&P

SUMMARY

In addition to vertical time shifts commonly observed in time-lapse seismic images, horizontal displacements are apparent as well. These apparent horizontal displacements may be small relatively to seismic wavelengths, perhaps only 5 m at depths of 5 km, but they consistently suggest an outward lateral expansion of images away from a compacting reservoir.

It is well known that apparent vertical displacements are caused mostly by a decrease in seismic wave velocities above compacting reservoirs. Those same velocity changes contribute to horizontal displacements. This contribution can be computed from the velocity changes that, in turn, can be estimated from measured vertical displacements. Horizontal displacements computed in this way are similar to those measured, and this similarity suggests that horizontal as well as vertical displacements may be largely due to velocity changes.

INTRODUCTION

Physical displacements of rocks during reservoir compaction cause *apparent displacements* in time-lapse seismic images. Figures 1a and 1b illustrate an example of apparent vertical displacements (time shifts) measured from two seismic images of a high-pressure high-temperature reservoir in the North Sea.

Figure 1a shows three orthogonal slices from a 3-D seismic image acquired in 2002. Lines in each of the three slices indicate where they intersect in 3-D. The one point where all three slices intersect lies just beneath the target reservoir. To monitor changes in that reservoir, a second 3-D seismic image (not shown) was acquired in 2004. By cross-correlating these two 3-D images for many overlapping windows, we obtain estimates of apparent vertical displacements δt like those shown in Figure 1b.

These measured apparent vertical displacements δt are mostly positive; that is, vertical two-way reflection times generally increase from 2002 to 2004. Hatchell and Bourne (2005a, 2005b) show that such increases are caused mostly by a decrease in seismic wave velocity in rocks above the reservoir as those rocks are stretched by reservoir compaction.

In this sense, Figure 1b is an image of a low-velocity lens. And if not accounted for in seismic migration (as it was not here), this lens above the reservoir will cause *apparent horizontal displacements* that may obscure any concurrent physical horizontal displacements of subsurface rocks.

Displacements in 3-D are vectors with three components - vertical, inline and crossline - and with careful processing we can measure all three. Figures 1c and 1d show measured inline (δx) and crossline (δy) components of apparent displacements corresponding to the same two images acquired in 2002 and 2004. Like the vertical displacements in Figure 1b, these apparent lateral displacements are not constant. Both δx and δy vary as functions of vertical time t , inline distance x and crossline distance y . Together the three components δt , δx and δy comprise a 3-D apparent displacement vector field.

Figures 1c and 1d suggest that apparent displacements in the inline and

crossline directions are less consistent than those in the vertical direction. Most measured lateral displacements are less than 5 m, which is relatively small compared with horizontal sampling intervals (inline and crossline trace spacings) of 25 m.

But the largest of these measured lateral displacements appear to be spatially correlated with the reservoir location. Specifically, they imply that, near the reservoir, *the seismic image is expanding horizontally*.

In this paper we show that much of this apparent horizontal expansion can be explained by the low-velocity lens above the reservoir in 2004. Using the concept of image rays, we show that horizontal displacements like those in Figures 1c and 1d are consistent with an expected expansion outward, away from the center of the reservoir where vertical compaction is largest.

Moreover, from the measured vertical displacements displayed in Figure 1b, we can estimate the location, size and shape of the low-velocity lens and then compute expected magnitudes of corresponding horizontal displacements. We show below that those computed magnitudes are approximately 5 m near the reservoir, with a spatial pattern that is consistent with measured displacements.

WHICH WAY?

The processing used to measure the apparent displacements shown in Figures 1b–1d began with local 3-D prediction-error filtering of the two 3-D seismic images (Hale, 2007). This processing was *local* in that for each image sample we computed a different 3-D prediction-error filter from a 3-D autocorrelation of only nearby samples. When applied to the 3-D seismic image of Figure 1a, local 3-D prediction-error filtering yields the less coherent image displayed in Figure 2.

As expected, local prediction-error filtering has attenuated laterally coherent features, while preserving those features in our images that best enable us to resolve all three components of displacement. Without this filtering, displacements are well defined in only those directions perpendicular to features that (in seismic images) tend to be planar or linear within small cross-correlation windows. Local 3-D prediction-error filtering attenuates such locally predictable features, thereby leaving only a less predictable, more random texture from which we can measure three components of displacement.

Furthermore, by highlighting point-like features that tend to scatter seismic waves in all directions, this filtering simplifies our analysis of lateral displacements. We need not be concerned with specular reflections from subsurface interfaces dipping at various angles. Instead, we need only consider diffractions from scattering points.

Figure 3 illustrates diffractions in 2002 and 2004 for a single stationary point in the subsurface. In this example, we assume that the point is located on the left side of a compacting reservoir. Compaction causes a dilation of rocks above the reservoir and a corresponding decrease in velocity, so that velocity in 2004 tends to decrease from left to right above this point.

This left-to-right decrease in velocity will cause a right-to-left displacement of diffractions. Velocities directly above the diffracting

Apparent horizontal displacements

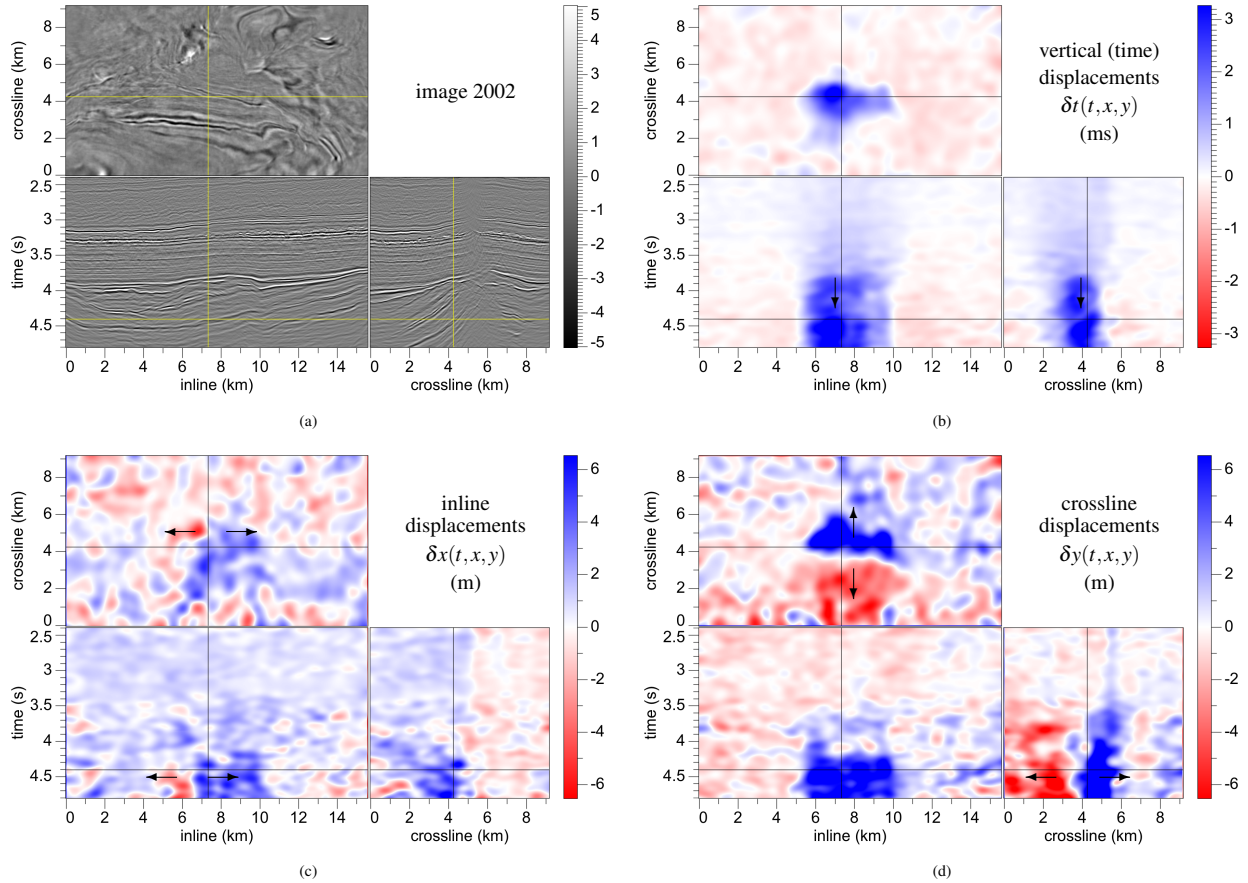


Figure 1: Slices (a) of a 3-D seismic image recorded in 2002. A second image (not shown) was recorded in 2004. Vertical (b) components of apparent displacement are measured in ms; inline (c) and crossline (d) components are measured in m. Crosshairs in each slice show the locations of the other two slices.

point are lower in 2004, so that seismic waves propagating there will arrive at the surface later than they did in 2002. The shortest two-way traveltime in 2004 corresponds to an image ray (Hubral, 1975, 1977; Larner et al., 1981) that emerges to the left of the diffracting point, where velocity is higher. Therefore, where velocity decreases from left to right, the peaks of diffractions will shift from right to left.

Now imagine the effect of migration on these two diffractions, where the same migration velocities (the 2002 velocities) are used for both. We would typically use the same velocities, in part because we might not yet know how velocities have changed in 2004. Migration will collapse the diffractions to construct point-like features in migrated images. In migrated time sections, each imaged point will appear at the apex of its corresponding diffraction curve. The point in 2004 will be imaged to the left of the point in 2002.

Assuming that the point in Figure 3 was correctly imaged in 2002, then that same point will be incorrectly imaged in 2004 to the left of its true location.

On the opposite side of the reservoir, where velocity in 2004 decreases from right to left, point-like features in 2004 will be imaged to the right of their true locations. Therefore, the effect of the low-velocity lens above the reservoir in 2004 is an apparent expansion of the image beneath that lens.

Of course, the horizontal displacement of diffractions in Figure 3 is greatly exaggerated. Recall that measured displacements are roughly 5 m at depths of 5 km. This illustration explains only the direction, not the magnitude, of the displacements of diffractions and imaged points that we may expect as velocity above a compacting reservoir decreases.

HOW FAR?

To quantify apparent horizontal displacements, we must first quantify the change in velocity from 2002 to 2004, and then compute image rays for 2004 like the one shown in Figure 3. We can estimate the change in velocity from the apparent vertical displacements in time δt shown in Figure 1b.

Let $d_z = v dt$ denote the distance that a seismic wave in 2002 travels vertically downward with velocity v in time Δt . Assuming that changes δz , δv and δt from 2002 to 2004 are small, we have $d(\delta z) = \delta v dt + v d(\delta t)$ and

$$\epsilon_{zz} \equiv \frac{d(\delta z)}{d_z} = \frac{\delta v}{v} + \frac{d(\delta t)}{dt}. \quad (1)$$

Here $\epsilon_{zz} \equiv d(\delta z)/d_z$ denotes vertical strain. The quantity $d(\delta t)/dt$ is sometimes called *time strain* (e.g., Rickett, 2006). An alternative

Apparent horizontal displacements

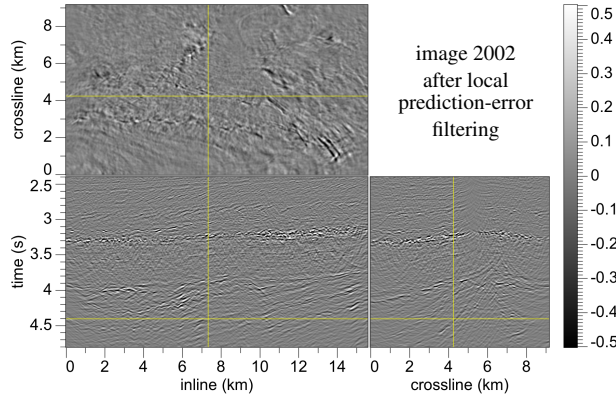


Figure 2: Slices of the image of Figure 1a after local 3-D prediction-error filtering to highlight scattering points. (Note that the amplitude scale is ten times smaller in this figure.) The same filtering was also applied to a second image (not shown) recorded in 2004.

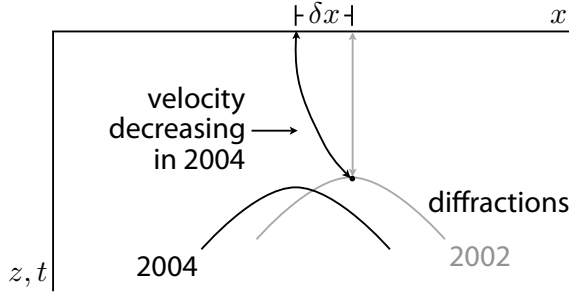


Figure 3: Image rays and diffractions in 2002 and 2004 for a single diffracting point located below and left of a low-velocity lens present only in 2004. Above this point, velocity in 2004 decreases from left to right. Horizontal displacement δx here is greatly exaggerated. All image rays are vertical at the surface.

phrase that extends well to three components of apparent displacement is *apparent strain*.

Hatchell and Bourne (2005a, 2005b) show that the fractional change in velocity is well approximated by $\delta v/v = -R\epsilon_{zz}$, where $R \approx 5$ for rocks above many different compacting reservoirs around the world. With equation 1, we see that this same fractional change in velocity is also proportional to apparent vertical strain:

$$\frac{\delta v}{v} = -\frac{R}{1+R} \frac{d(\delta t)}{dt}. \quad (2)$$

In other words, given measured apparent displacements $\delta t(t, x, y)$ like those in Figure 1b and interval velocities $v(t)$ measured in 2002, we can estimate changes in velocity $\delta v(t, x, y)$.

With $\delta v(t, x, y)$, we may then use image ray tracing to estimate apparent horizontal displacements $\delta x(t, x, y)$ or $\delta y(t, x, y)$. This ray tracing is greatly simplified by the observation that, because velocity changes $\delta v(t, x, y)$ are small, image rays vertical at the surface remain essentially vertical in the subsurface. Apparent displacements δx and δy are small fractions of reservoir depths, and are well approximated by small perturbations to vertical image rays.

Our derivation of time-lapse perturbations to image ray tracing equa-

tions is too lengthy to provide here, but is analogous to that used to obtain equation 1. Combining those perturbations with equation 2, we obtain the following expressions for horizontal displacements $\delta x(t, x, y)$ and $\delta y(t, x, y)$:

$$\begin{aligned} \delta x &= -\frac{R}{1+R} \int_0^t \frac{v^2}{4} \frac{\partial(\delta t)}{\partial x} dt, \\ \delta y &= -\frac{R}{1+R} \int_0^t \frac{v^2}{4} \frac{\partial(\delta t)}{\partial y} dt. \end{aligned} \quad (3)$$

In both of these expressions, t denotes the same two-way vertical traveltimes labeled in Figures 1.

As suggested by Cox and Hatchell (2008), we may express both lateral and vertical displacements in terms of a single “time-shift potential” function $\phi = \phi(t, x, y)$ defined by

$$\phi \equiv -\int_0^t \frac{v^2}{4} \delta t dt, \quad (4)$$

so that

$$\delta x = \frac{R}{1+R} \frac{\partial \phi}{\partial x}, \quad \delta y = \frac{R}{1+R} \frac{\partial \phi}{\partial y}, \quad \delta t = -\frac{4}{v^2} \frac{\partial \phi}{\partial t}. \quad (5)$$

Equations 4 and 5 provide rather simple relationships between apparent horizontal displacements $\delta x(t, x, y)$ and $\delta y(t, x, y)$ and apparent vertical displacements $\delta t(t, x, y)$. Because we have measured all three components of displacement (displayed in Figures 1b–1d), we can test these relationships.

TESTING

Equations 4 and 5 enable us to test the hypothesis that apparent horizontal displacements, like apparent vertical displacements, are caused mostly by decreases in seismic velocities above a compacting reservoir. If this hypothesis is valid, then $\delta x(t, x, y)$ and $\delta y(t, x, y)$ that we compute via equations 4 and 5 from measured $\delta t(t, x, y)$ should be comparable to our measured $\delta x(t, x, y)$ and $\delta y(t, x, y)$. Discrepancies might suggest other explanations not considered here, such as physical horizontal displacements or changes in seismic anisotropy, as well as errors in our measurements.

Any $\delta x(t, x, y)$ and $\delta y(t, x, y)$ that we compute from measured $\delta t(t, x, y)$ will of course have errors. In this respect, the integration over time t in equation 4 has both advantages and disadvantages. On the one hand, this integration performs a smoothing that will tend to attenuate errors in $\delta t(t, x, y)$ that are amplified by lateral derivatives $\partial \phi / \partial x$ and $\partial \phi / \partial y$. On the other hand, integration enables errors in $\delta t(t, x, y)$ for small times to alter the $\delta x(t, x, y)$ or $\delta y(t, x, y)$ computed for all times.

Unfortunately, errors in $\delta t(t, x, y)$ can be large for small times t , where image quality is often degraded as seismograms recorded with large source-receiver offsets are muted. In time-lapse imaging, any variations in seismic acquisition or muting patterns have a more significant effect on earlier reflections than on later ones. Therefore, we should generally avoid integrating from time $t = 0$ in equation 4.

Although not displayed in Figure 1b, measured vertical displacements δt for times $t = 0$ to 2.4 s are negligible in this example, except for a brief range (less than 100 ms) of small times t where the errors cited above are largest. Therefore, when computing ϕ via equation 4, we replaced the lower limits of integration $t = 0$ with $t = 2.4$ s, the beginning of the time window displayed in Figures 1.

Apparent horizontal displacements

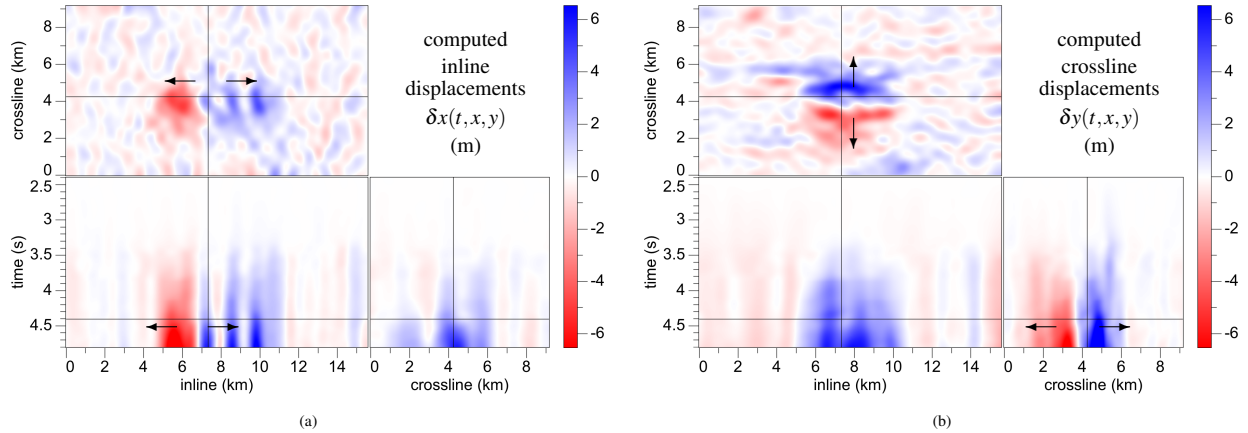


Figure 4: Computed (a) inline and (b) crossline components of apparent displacement vectors, in m. Compare with Figures 1c and 1d.

In addition to measured apparent vertical displacements δt , application of equations 4 and 5 requires estimates for interval velocities $v(t)$ and R . We estimated the function $v(t)$ using depths and times measured in a checkshot survey. The parameter R is more difficult to estimate, but for large values of $R \approx 5$ the ratio $R/(1+R)$ is fairly insensitive to uncertainties in R . We assumed a constant $R = 5$.

For the sampled images in this example, we used a simple sum to approximate the integral over time t in equation 4, and a two-sample centered finite-difference approximation to the partial derivatives $\partial\phi/\partial x$ and $\partial\phi/\partial y$ in equations 5. The apparent horizontal displacements computed in this way are displayed in Figures 4.

Computed horizontal displacements displayed in Figures 4a and 4b are clearly not the same as the measured horizontal displacements in Figures 1c and 1d. In particular, computed horizontal displacements are noticeably smoother in time than measured horizontal displacements.

Still, the spatial patterns of the larger displacements are comparable. Both computed and measured displacements imply an apparent lateral expansion. And near the reservoir magnitudes of computed horizontal displacements are approximately 5 m, consistent with measured horizontal displacements.

Moreover, although our derivation and computations here are different, the computed horizontal displacements shown in Figures 4a and 4b are generally consistent with those shown by Cox and Hatchell (2008). They also show that displacements δx and δy computed from measured δt are comparable to those computed by ray-tracing for a velocity function $v + \delta v$ estimated from a geomechanical model.

CONCLUSIONS

This research began with the unexpected observation that time-lapse seismic images appear to expand laterally away from a compacting reservoir. The simplest explanation for these apparent horizontal displacements is that they are caused primarily by a decrease in seismic wave velocities above the reservoir.

That decrease in velocities is well understood to be largely responsible for the apparent vertical displacements that we today measure routinely in time-lapse imaging. The concept is simple. Waves that travel through thick layers of rocks with velocities that have decreased slightly will arrive slightly later in time.

The extension of this concept to horizontal displacements is only a bit more complex, requiring only an understanding of how waves are focused by a low-velocity lens, and how that focusing alters seismic images that have not been processed to account for it.

To account for changes in velocity, we must first quantify them. The method presented in this paper uses lateral derivatives of measured apparent vertical displacements to estimate relevant lateral changes in velocity. Image ray approximations then provide a simple method for computing apparent horizontal displacements in time-lapse seismic images.

Our ability to compute apparent horizontal displacements caused by velocity changes leads to an interesting question. If we subtract any horizontal displacements that we compute from those we measure, are we left with physical horizontal displacements?

Before we can answer this question, we must better understand the accuracy with which we can measure displacements from seismic images, as well as the spatial resolution of those measurements. The processing used here was tuned to enable measurements of all three components of displacements, and care was taken to maximize the fidelity of each step in this processing. But the displacements we measure may be small fractions of seismic wavelengths, and a tradeoff between accuracy and resolution is unavoidable.

The results shown in this paper suggest that future work to improve our understanding of accuracy and resolution in time-lapse seismic imaging is worthwhile. We should ideally measure displacements from unstacked seismic images, because the effects of a low-velocity lens will vary for different source-receiver offsets. We might also consider additional contributions to apparent lateral displacements, such as those resulting from changes in seismic anisotropy. Similarities and differences like those shown here between computed and measured horizontal displacements are interesting. It remains to be seen whether they can be made meaningful.

ACKNOWLEDGMENTS

We thank Shell U.K. Limited and the Shearwater partnership (Shell, BP, and ExxonMobil) for providing access to their time-lapse seismic images and permission to publish results derived from them.

Apparent horizontal displacements

REFERENCES

- Cox, B. and P. Hatchell, 2008, Straightening out lateral shifts on time-lapse seismic data: First Break, May, 2008 (submitted).
- Hale, D., 2007, A method for estimating apparent displacement vectors from time-lapse seismic images: 77th Annual International Meeting, SEG, Expanded Abstracts, 2939–2943.
- Hatchell, P. and S. Bourne, 2005a, Measuring reservoir compaction using time-lapse timeshifts: 75th Annual International Meeting, SEG, Expanded Abstracts, 2500–2504.
- Hatchell, P. and S. Bourne, 2005b, Rocks under strain: Strain-induced time-lapse time shifts are observed for depleting reservoirs: *The Leading Edge*, **24**, 1222–1225.
- Hubral, P. 1975, Locating a diffractor below plane layers of constant interval velocity and varying dip: *Geophysical Prospecting*, **23**, 313–322.
- Hubral, P. 1977, Time migration — Some ray theoretical aspects: *Geophysical Prospecting*, **25**, 738–745.
- Larner, K.L., L. Hatton, B.S. Gibson, and I. Hsu, 1981, Depth migration of imaged time sections: *Geophysics*, **46**, 734–750.
- Rickett, J.E., L. Duranti, T. Hudson, and N. Hodgson, 2006, Compaction and 4-D time strain at the Genesis Field: 76th Annual International Meeting, SEG, Expanded Abstracts, 3215–3219.